Inorg. Chem. **2005**, *44*, 2596–2605

Mononuclear Titanium(IV)–Citrate Complexes from Aqueous Solutions: pH-Specific Synthesis and Structural and Spectroscopic Studies in Relevance to Aqueous Titanium(IV)–Citrate Speciation

E. T. Kefalas,[†] P. Panagiotidis,[‡] C. P. Raptopoulou,[§] A. Terzis,[§] T. Mavromoustakos,[||] and A. Salifoglou*[,‡]

Department of Chemical Engineering, Laboratory of Inorganic Chemistry, Aristotle University of Thessaloniki, Thessaloniki 54124, Greece, Chemical Process Engineering Research Institute, Thermi, Thessaloniki 57001, Greece, Department of Chemistry, University of Crete, Heraklion 71409, Greece, Institute of Materials Science, NCSR "Demokritos", Aghia Paraskevi 15310, Attiki, Greece, and Institute of Organic and Pharmaceutical Chemistry, National Hellenic Research Foundation, Athens 11635, Greece

Received June 3, 2004

Titanium is a metal frequently employed in a plethora of materials supporting medical applications. In an effort to comprehend the involvement of titanium in requisite biological interactions with physiological ligands, synthetic efforts were launched targeting aqueous soluble species of Ti(IV). To this end, aqueous reactions of $TiCl_4$ with citric acid afforded expediently, under pH-specific conditions, the colorless crystalline materials $Na_6[Ti(C_6H_{4.5}O_7)_2(C_6H_5O_7)]\cdot 16H_2O$ (**1**) and $Na_3(NH_4)_3[Ti(C_6H_{4.5}O_7)_2(C_6H_5O_7)]\cdot 9H_2O$ (**2**). Complexes **1** and **2** were characterized by elemental analysis, FT-IR, ^{13}C-MAS solid state and solution NMR, cyclic voltammetry, and X-ray crystallography. **1** crystallizes in the triclinic space group $P\bar{1}$, with $a = 15.511(9)$ Å, $b = 15.58(1)$ Å, $c = 9.848(5)$ Å, $\alpha = 85.35(2)°$, $\beta = 76.53(2)°$, $\gamma = 61.97(2)°$, $V = 2042(2)$ Å^3, and $Z = 2$. **2** crystallizes in the triclinic space group $P\bar{1}$, with $a = 12.437(5)$ Å, $b = 12.440(5)$ Å, $c = 12.041(5)$ Å, $\alpha = 83.08(2)°$, $\beta = 81.43(2)°$, $\gamma = 67.45(2)°$, $V = 1697(2)$ Å^3, and $Z = 2$. The X-ray structures of **1** and **2** reveal the presence of a mononuclear complex, with Ti(IV) coordinated to three citrate ligands in a distorted octahedral geometry around Ti(IV). The citrates employ their central alkoxide and carboxylate groups to bind Ti(V), while the terminal carboxylates stay away from the $Ti^{IV}O_6$ core. Worth noting in **1** and **2** is the similar mode of coordination but variable degree of protonation of the bound citrates, with the locus of (de)protonation being the noncoordinating terminal carboxylates. As a result, this work suggests the presence of a number of different Ti(IV)–citrate species of the same nuclearity and coordination geometry as a function of pH. This is consistent with the so far existing pool of mononuclear Ti(IV)–citrate species and provides a logical account of the aqueous speciation in the requisite binary system. Such information is vital in trying to delineate the interactions of soluble and bioavailable Ti(IV) forms promoting biological interactions in humans. To this end, chemical properties, structural attributes, and speciation links to potential ensuing biological effects are dwelled on.

Introduction

Titanium is a transition metal which has found use in a diverse spectrum of scientific disciplines.[1] Notable is the use of Ti(III)−citrate in biochemical research, where it is employed as a reducing agent in probing mechanistic functional connections in key enzymes (i.e. nitrogenase) of metallobiological processes in lower organisms.[2] Equally extensive is the use of titanium metal in the manufacturing

* Author to whom correspondence should be addressed. E-mail: salif@auth.gr. Tel: +30-2310-996-179. Fax: +30-2310-996-196.
[†] University of Crete.
[‡] Aristotle University of Thessaloniki and Chemical Process Engineering Research Institute.
[§] NCSR "Demokritos".
[||] National Hellenic Research Foundation.

(1) (a) Biehl, V.; Wack, T.; Winter, S.; Seyfert, U. T.; Breme, J. *Biomol. Eng.* **2002**, *19*, 97−101. (b) Thull, R. *Biomol. Eng.* **2002**, *19*, 43−50. (c) Paladino, J.; Stimac, D.; Rotim, K.; Pirker, N.; Stimac, A. *Minim. Invas. Neurosur.* **2000**, *43*, 72−74. (d) Sumi, Y.; Hattori, H.; Hayashi, K.; Ueda, M. *J. Endodont.* **1997**, *23*, 21−23. (e) Yuan, Y.; Li, X.; Sun, J.; Ding, K. *J. Am. Chem. Soc.* **2002**, *124*, 14866−14867. (f) Kii, S.; Maruoka, K. *Chirality* **2003**, *15*, 68−70.

10.1021/ic049276o CCC: $30.25
Published on Web 03/12/2005

of ceramic materials,[3] alloys, and composites, employed in surgical rectification devices frequently implanted in patients with orthopedic problems,[4] dental fillings,[5] and other applications.[6] Inescapably, contact of that metal ion with biological tissues and surrounding fluids results in titanium solubilization and further entry in (bio)chemical interactions, leading to short- and long-term manifestations exemplified through symptoms of clinical rejection or toxic effects. A number of studies have been conducted[7] aiming to rationalize the macroscopic involvement of titanium in clinical symptomatologies associated with the use of titanium-containing prosthetic materials[8] inducing clinical effects (e.g. inflammatory processes) and affecting human physiology.[9]

In view of the picture formulated by macroscopic chemical events unfolding in the presence of titanium, the urgent need arises to understand the bioinorganic chemistry underlying the observed effects linked to physiological aberrations. Such a feat requires perusal of the intricate interactions between bioavailable titanium and biological molecules with which it comes in contact. In turn, that entails in-depth perusal of basic chemical interactions relating to the distribution of soluble aqueous titanium forms as a function of pH and concentration of the interacting partners. The latter include both low and high molecular mass biomolecules. Hence, structural speciation arises as an important issue in need of delineation. To this end, our efforts have concentrated on resolving questions related to the interaction of titanium with low molecular mass ligands, focusing specifically on the physiological α-hydroxycarboxylic acids, with a key representative being citric acid. The latter exists in human plasma at a concentration of 0.1 mM. It is known to promote metal ion solubilization and to further contribute to their absorption by biological tissues.[10] Cognizant of the limited number of known structurally characterized species of titanium with citrates,[11−13] we (a) report herein on the synthesis, isolation, and spectroscopic and structural characterization of new Ti(IV)−citrate species from aqueous media and (b) present arguments associating pH variants of those species in the aqueous speciation of the binary Ti(IV)−citrate system as well as its potential implications on further interactions in biological fluids.

Experimental Section

Materials and Methods. All experiments were carried out in the open air. Nanopure quality water was used for all reactions. $TiCl_4$ and anhydrous citric acid were purchased from Aldrich. Ammonia was supplied by Fluka.

Physical Measurements. FT-infrared measurements were taken on a Perkin-Elmer 1760X FT-infrared spectrometer. Elemental analyses were performed by Quantitative Technologies, Inc.

(a) Solid-State NMR. The high-resolution solid-state ^{13}C magic angle spinning (MAS) NMR spectra were measured at 100.63 MHz, on a Bruker MSL400 NMR spectrometer, capable of high-power ^1H-decoupling. The spinning rate used for $^1H-^{13}C$ cross polarization and magic angle spinning experiments was 5 kHz at ambient temperature (25 °C). Each solid-state spectrum was a result of the accumulation of 200 scans. The recycle delay used was 4 s, the 90° pulse was 5 μs, and the contact time was 1 ms. All solid-state spectra were referenced to adamantane, which showed two peaks at 26.5 and 37.6 ppm, respectively, and to the external reference of TMS.

(b) Solution NMR. The samples for solution NMR studies were prepared by dissolving the crystalline complexes in D_2O, at concentrations in the range 0.02−0.10 M. NMR spectra were recorded on a Bruker AM360 (^1H and ^{13}C) spectrometer. Chemical shifts (δ) are reported in ppm relative to an internal reference of TMS.

(c) Electrochemical Measurements. Electrochemical measurements were carried out with a Uniscan Instruments Ltd. model PG580 potensiostat−galvanostat. The entire system was under computer control and supported by the appropriate computer software Ui Chem version 1.08RD, running on Windows. The electrochemical cell used had platinum (disk) working and auxiliary (wire) electrodes. As reference electrode, a saturated calomel electrode (SCE) was used. Thus, the derived potentials in the cyclic voltammetric measurements are referenced to the SCE reference electrode. The water used in the electrochemical measurements was of nanopure quality. KNO_3 was used as a supporting electrolyte. Normal concentrations used were 1−6 mM in electroanalyte and 0.1 M in supporting electrolyte. Purified argon was used to purge the solutions prior to the electrochemical measurements.

Preparation of Complex $Na_6[Ti(C_6H_{4.5}O_7)_2(C_6H_5O_7)]\cdot 16H_2O$ (1). A quantity of anhydrous citric acid (0.58 g, 3.0 mmol) was placed in a flask and dissolved in 2 mL of H_2O. Subsequently, $TiCl_4$ (0.20 g, 1.0 mmol) was added slowly and under continuous stirring. Aqueous sodium hydroxide was then added slowly to adjust the pH to a final value of ∼6.0. Initially, the resulting reaction mixture was slightly cloudy. Filtration followed, and the arising

(2) Schneider, K.; Müller, A.; Krahn, E.; Hagen, W. R.; Wassink, H.; Knüttel, K.-H. *Eur. J. Biochem.* **1995**, *230*, 666−675.

(3) (a) Hung, K.-M.; Yang, W.-D. *Mater. Sci. Eng., A* **2003**, *351*, 70−80. (b) Zhang, Y.; Kuang, A.; Chan, H. L.-W. *Microelectr. Eng.* **2003**, *66*, 918−925. c) Kong, L. B.; Ma, J.; Zhang, R. F.; Zhu, W.; Tan, O. K. *Mater. Lett.* **2002**, *55*, 370−377. (c) Chandler, C. D.; Roger, C.; Hampden-Smith, S. J. *Chem. Rev.* **1993**, *93*, 1205−1241.

(4) Bardos, D. In *Titanium and Zirconium Alloys in Orthopedic Applications*; Altobelli, D. E., Gresser, J. D., Schwartz, E. R., Trantolo, D. J., Wise, D. L., Yaszemski, M. J., Eds.; Encyclopedic Handbook of Biomaterials and Bioengineering; Marcel Dekker: New York, 1995; pp 509−548.

(5) (a) Degidi, M.; Petrone, G.; Iezzi, G.; Piattelli, A. *Clin. Implant. Dent. Relat. Res.* **2002**, *4*, 110−114. (b) Knabe, C.; Klar, F.; Fitzner, R.; Radlanski, R. J.; Gross, U. *Biomaterials* **2002**, *23*, 3235−3245.

(6) (a) Shimizu, H.; Habu, T.; Takada, Y.; Watanabe, K.; Okuno, O.; Okabe, T. *Biomaterials* **2002**, *23*, 2275−2281. (b) Moroni, A.; Faldini, C.; Rocca, M.; Stea, S.; Giannini, S. *J. Orthop. Trauma* **2002**, *16*, 257−263. (c) Oka, M. *J. Orthop. Sci.* **2001**, *6*, 448−456.

(7) (a) Schwartz, Z.; Lohmann, C. H.; Vocke, A. K.; Sylvia, V. L.; Cochran, D. L.; Dean, D. D.; Boyan, B. D. *J. Biomed. Mater. Res.* **2001**, *56*, 417−426. (b) Takei, H.; Pioletti, D. P.; Kwon, S. Y.; Sung, K.-L. P. *J. Biomed. Mater. Res.* **2000**, *52*, 382−387. (c) Wang, J. Y.; Tsukayama, D. T.; Wicklund, B. H.; Gustilo, R. B. *J. Biomed. Mater. Res.* **1996**, *32*, 655−661.

(8) Suzuki, R.; Frangos, J. A. *Clin. Orthop. Relat. Res.* **2000**, *372*, 280−289.

(9) (a) Tengvall, P.; Elwing, H.; Sjoqvist, L.; Lundstrom, I.; Bjursten, L. *Biomaterials* **1989**, *10*, 118−120. (b) Tengvall, P.; Lundstrom, I.; Sjoqvist, L.; Elwing, H.; Bjursten, L. *Biomaterials* **1989**, *10*, 166−175. (c) Tengvall, P.; Walivaara, B.; Westerling, J.; Lundstrom, I. *J. Colloid Interface Sci.* **1991**, *143*, 589−592.

(10) (a) Martin, R. B. *Inorg. Biochem.* **1986**, *28*, 181−187. (b) Glusker, J. P. *Acc. Chem. Res.* **1980**, *13*, 345−352.

(11) Kakihana, M.; Tada, M.; Shiro, M.; Petrykin, V.; Osada, M.; Nakamura, Y. *Inorg. Chem.* **2001**, *40*, 891−894.

(12) Dakanali, M.; Kefalas, E. T.; Raptopoulou, C. P.; Terzis, A.; Voyiatzis, G.; Kyrikou, I.; Mavromoustakos, T.; Salifoglou, A. *Inorg. Chem.* **2003**, *42*, 4632−4639.

(13) Zhou, Z.-H.; Deng, Y.-F.; Jiang, Y.-Q.; Wan, H.-L.; Ng, S.-W. *J. Chem. Soc., Dalton Trans.* **2003**, 2636−2638.

Table 1. Summary of Crystal, Intensity Collection, and Refinement Data for $Na_6[Ti(C_6H_{4.5}O_7)_2(C_6H_5O_7)]\cdot 16H_2O$ (**1**) and $Na_3(NH_4)_3[Ti(C_6H_{4.5}O_7)_2(C_6H_5O_7)]\cdot 9H_2O$ (**2**)

	1	2
formula	$C_{18}H_{46}Na_6O_{37}Ti$	$C_{18}H_{44}N_3Na_3O_{30}Ti$
fw	1040.39	899.43
T (K)	298	298
radiatn (wavelength, Å)	Mo Kα (0.710 73)	Cu Kα (1.5418)
space group	$P\bar{1}$	$P\bar{1}$
a (Å)	15.511(9)	12.437(5)
b (Å)	15.58(1)	12.440(5)
c (Å)	9.848(5)	12.041(5)
α (deg)	85.35(2)	83.08(2)
β (deg)	76.53(2)	81.43(2)
γ (deg)	61.97(2)	67.45(2)
V (Å^3)	2042(2)	1697(2)
Z	2	2
D_{calcd}/D_{measd} (Mg m^{-3})	1.692/1.70	1.760/1.77
abs coeff (μ) (mm^{-1})	0.391	3.607
range of h, k, l	$-17 \rightarrow 18$, $-17 \rightarrow 18$, $0 \rightarrow 11$	$-13 \rightarrow 13$, $-13 \rightarrow 13$, $0 \rightarrow 13$
goodness-of-fit on F^2	1.024	1.043
R indices[a]	$R = 0.0623$, $R_w = 0.1628$[b]	$R = 0.0636$, $R_w = 0.1762$[c]

[a] R values are based on F values; R_w values are based on F^2. $R = \Sigma||F_o| - |F_c||/\Sigma(|F_o|)$; $R_w = \sqrt{\Sigma[w(F_o^2 - F_c^2)^2]/\Sigma[w(F_o^2)^2]}$. [b] 5453 reflections with $I > 2\sigma(I)$. [c] 3771 reflections with $I > 2\sigma(I)$.

clear solution was placed in the refrigerator overnight. Addition of cold ethanol at 4 °C resulted after several days in the deposition of a colorless crystalline material. The product was isolated by filtration and dried in vacuo. Yield: 0.45 g (45%). Anal. Calcd for **1**, $Na_6[Ti(C_6H_{4.5}O_7)_2(C_6H_5O_7)]\cdot 16H_2O$ ($C_{18}H_{46}Na_6O_{37}Ti$, MW = 1040.39): C, 20.76; H, 4.42; Na, 13.26. Found: C, 20.79; H, 4.33; Na, 13.49.

Preparation of Complex $Na_3(NH_4)_3[Ti(C_6H_{4.5}O_7)_2(C_6H_5O_7)]\cdot 9H_2O$ (2). A quantity of anhydrous citric acid (0.58 g, 3.0 mmol) was placed in a flask and dissolved in 2 mL of H_2O. Subsequently, $TiCl_4$ (0.20 g, 1.0 mmol) was added slowly and under continuous stirring. Equal amounts of aqueous ammonia and sodium hydroxide were then added slowly to adjust the pH to a final value of ~6.0. Initially, the resulting reaction mixture was slightly cloudy. Filtration followed, and the arising clear solution was placed in the refrigerator overnight. Addition of cold ethanol at 4 °C resulted after 1 month in the deposition of a colorless crystalline material. The product was isolated by filtration and dried in vacuo. Yield: 0.78 g (29%). Anal. Calcd for **1**, $Na_3(NH_4)_3[Ti(C_6H_{4.5}O_7)_2(C_6H_5O_7)]\cdot 9H_2O$ ($C_{18}H_{44}Na_3O_{30}N_3Ti$, MW = 899.43): C, 24.10; H, 4.89; N, 4.67. Found: C, 24.65; H, 4.82; N, 4.72.

X-ray Crystallography. Crystal Structure Determination. X-ray-quality crystals of compounds **1** and **2** were grown from water−ethanol mixtures. A single crystal, with dimensions 0.03 × 0.15 × 0.40 mm (**1**), was mounted on a Crystal Logic dual-goniometer diffractometer, using graphite-monochromated Mo Kα radiation. Unit cell dimensions for **1** were determined and refined by using the angular settings of 25 automatically centered reflections in the range $11 < 2\theta < 23°$. A single crystal, with dimensions 0.04 × 0.10 × 0.35 mm (**2**), was mounted on a $P2_1$ Nicolet diffractometer upgraded by Crystal Logic, using graphite-monochromated Cu Kα radiation. Unit cell dimensions for **2** were determined and refined by using the angular settings of 25 automatically centered reflections in the range $22 < 2\theta < 54°$. Crystallographic details are given in Table 1. Intensity data were measured by using $\theta-2\theta$ scans. Three standard reflections were monitored every 97 reflections, over the course of data collection. They showed less than 3% variation and no decay. Lorentz and polarization corrections were applied by using Crystal Logic software. Further experimental crystallographic details for **1**: $2\theta_{max} = 49°$, scan speed 1.5°/min; scan range 2.2 + $\alpha_1\alpha_2$ separation; reflections collected/unique/used, 7203/6768 [$R_{int} = 0.0192$]/6768; 719 parameters refined; $(\Delta/\sigma)_{max} = 0.012$; $(\Delta\rho)_{max}/(\Delta\rho)_{min} = 0.823/-0.695$ e/Å^3; R/R_w (for all data), 0.0775/0.1825. Further experimental crystallographic details for **2**: $2\theta_{max} = 113.5°$, scan speed 3.0°/min; scan range 2.45 + $\alpha_1\alpha_2$ separation; reflections collected/unique/used, 4722/4486 [$R_{int} = 0.0552$]/4486; 560 parameters refined; $(\Delta/\sigma)_{max} = 0.014$; $(\Delta\rho)_{max}/(\Delta\rho)_{min} = 0.651/-1.062$ e/Å^3; R/R_w (for all data), 0.0750/0.1930.

The structures of **1** and **2** were solved by direct methods using SHELXS-86.[14] Refinement was achieved by full-matrix least-squares techniques on F^2 with SHELXL-93.[15] All non-H atoms in the structures of **1** and **2** were refined anisotropically. All H atoms of the citrate ligands in **1** were located by difference maps and were refined isotropically. Two of the sodium counterions, Na(5) and Na(6), are sitting on an inversion center of symmetry at (0, 0, 0.5) and (0.5, 0.5, 0), respectively. The 16 lattice water molecules were refined anisotropically; three of them were found disordered over two positions and were refined with occupancy factors of a total sum one. Most of the water H atoms were located by difference maps and were refined isotropically; the rest were not included in the refinement. The H atoms of the citrate carbon atoms in the structure of **2** were introduced at calculated positions as riding on bonded atoms. The rest were located by difference maps and were refined isotropically. The nine lattice water molecules and three ammonium counterions were refined anisotropically. Most of their hydrogen atoms were located by difference maps and were refined isotropically; the rest were not included in the refinement. Their characterization as water or ammonium molecules was based on their interatomic distances from the sodium counterions as well as their hydrogen-bonding interactions.

Results

Synthesis. The syntheses of complexes **1** and **2** were achieved expediently by reacting titanium tetrachloride and citric acid in water. Addition of aqueous sodium hydroxide in **1** and equal amounts of aqueous ammonia and sodium hydroxide in **2** raised the pH of the solution to ~6.0 and concurrently provided the necessary counterions for the subsequently derived anionic complex. The resulting colorless solution was treated with ethanol at 4 °C and afforded efficiently a colorless crystalline material.

The overall stoichiometric reaction leading to complexes **1** and **2** is shown schematically:

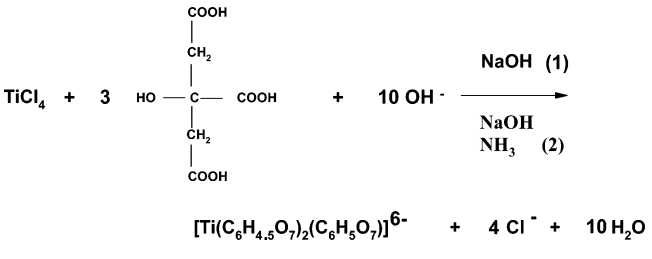

Elemental analyses on the isolated crystalline materials suggested the formulation $Na_6[Ti(C_6H_{4.5}O_7)_2(C_6H_5O_7)]\cdot$

(14) Sheldrick, G. M *SHELXS-86: Structure Solving Program*; University of Göttingen: Göttingen, Germany, 1986.
(15) Sheldrick, G. M *SHELXL-93: Structure Refinement Program*; University of Göttingen: Göttingen, Germany, 1993.

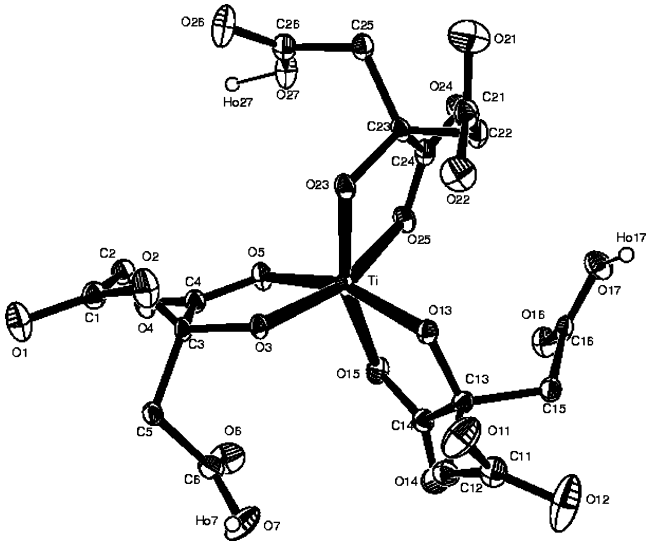

Figure 1. ORTEP structure of the $[Ti(C_6H_{4.5}O_7)_2(C_6H_5O_7)]^{6-}$ anion with the atom-labeling scheme in **1**. Thermal ellipsoids are drawn by ORTEP and represent 50% probability surfaces.

$16H_2O$ and $Na_3(NH_4)_3[Ti(C_6H_{4.5}O_7)_2(C_6H_5O_7)]\cdot 9H_2O$ for **1** and **2**, respectively. Complexes **1** and **2** in the crystalline form appear to be stable for long periods of time. They are insoluble in alcohols (CH_3OH, C_2H_5OH, and i-PrOH), acetonitrile, and dimethyl sulfoxide (DMSO), but they dissolve readily in water.

Description of the Crystal Structure of $Na_6[Ti(C_6H_{4.5}O_7)_2(C_6H_5O_7)]\cdot 16H_2O$ (1) and $Na_3(NH_4)_3[Ti(C_6H_{4.5}O_7)_2(C_6H_5O_7)]\cdot 9H_2O$ (2). The X-ray crystal structures of **1** and **2** consist of discrete anions and sodium cations. Complex **1** crystallizes in the triclinic space group $P\bar{1}$ with two molecules/unit cell. Complex **2** crystallizes in the triclinic space group $P\bar{1}$ with two molecules/unit cell. The ORTEP diagram of the anion in **1** is shown in Figure 1. A select list of interatomic distances and bond angles for **1** and **2** is given in Table 2. Due to the similarity of the anionic parts of the two compounds, the structures of **1** and **2** will be discussed together. The anionic complex in **1** is a mononuclear complex of titanium(IV) coordinated to three citrate ligands. The oxygens of the $Ti^{IV}O_6$ core unit originate in the alkoxide and the central carboxylate of each citrate ligand. Binding through those terminals ensures the formation of a stable five-membered metallacycle bestowing stability to the overall complex. Three such chelated ligands provide for coordination number 6 and a distorted octahedral coordination geometry around the central Ti(IV) ion. A similar picture is depicted in the case of complex **2**.

The Ti−O bond distances in **1** and **2** are in line with those in other Ti(IV) oxygen-containing complexes, like $K_3[Ti(C_6H_6O_7)_2(C_6H_5O_7)]\cdot K_4[Ti(C_6H_5O_7)_2(C_6H_6O_7)]\cdot 10H_2O$ (**3**) (1.871(2)−2.060(3) and 1.860(2)−2.048(3) Å for the two component complexes),[16] $(NH_4)_2[TiO(C_2O_4)_2]\cdot H_2O$ (**4**) (1.785(7)−1.855(6) Å),[17] $Cs_4[Ti_4O_4(C_6H_6NO_6)_4]\cdot 6H_2O$ (**5**) (1.74(1)−2.02(1) Å),[18] $K_2[Ti_2O_5(C_7H_3O_4N)_2]\cdot 5H_2O$ (**6**) (1.825(2)−2.183(7) Å),[19] $(NH_4)_8[Ti_4(C_6H_4O_7)_4(O_2)_4]\cdot 8H_2O$ (**7**) (1.863(1)−2.085(1) Å),[11] and $KMg_{1/2}[Ti(H_2cit)_3]\cdot 6H_2O$ (**8**) (1.865(1)−2.045(1) Å),[13] and $(NH_4)_4[Ti_2(O_2)_2(C_6H_4O_7)_4]\cdot 2H_2O$ (**9**) (1.852(2)−2.085(2) Å).[12] It appears that similar angles are observed in **1** and **2** and a number of $Ti^{IV}O_6$-core-containing complexes, exhibiting octahedral geometry around the titanium(IV) ions. Among such complexes included are **3** (78.7(1)−157.0(1) and 78.9(1)−159.8(1)° for the two anionic species, respectively), **4** (77.1(3)−171.2(12)°), and $KMg_{1/2}[Ti(H_2cit)_3]\cdot 6H_2O$ (**8**) (79.99(4)−156.52(5)°).[13]

Table 2. Bond Lengths (Å) and Angles (deg) in **1** and **2**

1		**2**	
	Distances		
Ti−O(3)	1.852(3)	Ti−O(3)	1.860(3)
Ti−O(23)	1.879(3)	Ti−O(23)	1.873(3)
Ti−O(13)	1.879(3)	Ti−O(13)	1.870(3)
Ti−O(25)	2.036(3)	Ti−O(25)	2.056(3)
Ti−O(15)	2.054(3)	Ti−O(15)	2.061(4)
Ti−O(5)	2.055(3)	Ti−O(5)	2.030(3)
	Angles		
O(3)−Ti−O(23)	98.6(1)	O(3)−Ti−O(23)	94.9(1)
O(3)−Ti−O(13)	97.9(1)	O(3)−Ti−O(13)	98.2(1)
O(23)−Ti−O(13)	95.6(1)	O(23)−Ti−O(13)	96.8(1)
O(3)−Ti−O(25)	159.2(1)	O(3)−Ti−O(25)	160.3(1)
O(23)−Ti−O(25)	78.7(1)	O(23)−Ti−O(25)	79.3(1)
O(13)−Ti−O(25)	102.9(1)	O(13)−Ti−O(25)	101.2(1)
O(3)−Ti−O(15)	103.2(1)	O(3)−Ti−O(15)	104.6(1)
O(23)−Ti−O(15)	158.2(1)	O(23)−Ti−O(15)	160.4(1)
O(13)−Ti−O(15)	79.3(1)	O(13)−Ti−O(15)	78.0(1)
O(25)−Ti−O(15)	81.8(1)	O(15)−Ti−O(25)	83.2(1)
O(3)−Ti−O(5)	78.6(1)	O(3)−Ti−O(5)	79.2(1)
O(23)−Ti−O(5)	103.2(1)	O(23)−Ti−O(5)	105.6(2)
O(13)−Ti−O(5)	161.2(1)	O(13)−Ti−O(5)	157.6(2)
O(25)−Ti−O(5)	82.0(1)	O(5)−Ti−O(25)	84.3(1)
O(15)−Ti−O(5)	83.5(1)	O(5)−Ti−O(15)	81.2(1)

The citrate ligands in the anion of **1** adopt a "bend" conformation (i.e. the carbon atoms C(1), C(2), C(3), C(5), and C(6) of the citrate backbone are not coplanar) upon binding to the titanium ion. In all three citrates, the carbon of the terminal deprotonated carboxylate is displaced by ∼1.1 Å out of the best mean plane of the remaining four carbon atoms defining the citrate backbone. The same observation is also true for the anion in **2** (the displacement of the terminal deprotonated carboxylate is 1.1 Å for C(6), 1.4 Å for C(16), and 0.97 Å for C(26)). In the anion of **1**, the central carboxylate plane O(4)−C(4)−O(5) for the first citrate is rotated ∼5.7° out of the O(3)−C(3)−C(4) plane, the central carboxylate plane O(14)−C(14)−O(15) for the second citrate is rotated ∼12.1° out of the O(13)−C(13)−C(14) plane, and the central carboxylate plane O(24)−C(24)−O(25) for the third citrate is rotated ∼3.8° out of the O(23)−C(23)−C(24) plane. The corresponding values for the anion in **2** are 6.2, 12.0, and 7.1°, respectively. These values are congruent with those seen in congener Ti(IV)−citrate complexes, suggesting a similar approach of the citrate ligands to the metal ions in the anionic assembly.[13,16]

The presence of protonated terminal carboxylates in the structure of **1** plays a key role in the development of its lattice

(16) Kefalas, E. T.; Raptopoulou, C. P.; Terzis, A.; Mavromoustakos, T.; Salifoglou, A. To be submitted for publication.
(17) Van de Velde, G. M. H.; Harkema, S.; Jellings, P. J. *Inorg. Chim. Acta* **1974**, *11*, 243−252.
(18) Wieghardt, K.; Quilitzsch, U.; Weiss, J.; Nuber, B. *Inorg. Chem.* **1980**, *19*, 2514−2519.
(19) Schwarzenbach, D. *Inorg. Chem.* **1970**, *9*, 2391−2397.

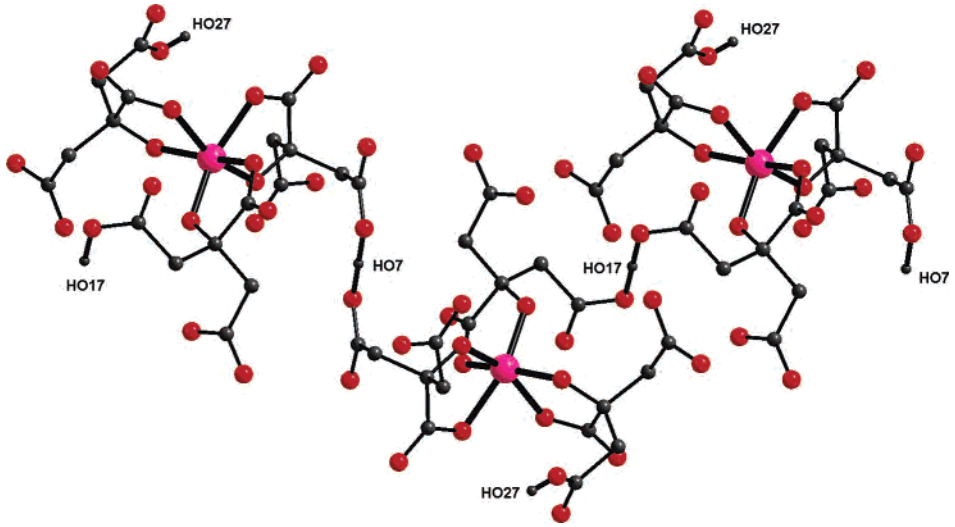

Figure 2. ORTEP plot of **1** showing the development of chains of the anions along the *b* axis through hydrogen-bonding interactions.

Table 3. Hydrogen Bonds in **1**

interaction	D···A (Å)	H···A (Å)	D−H···A (deg)	sym operation
O7−HO7···O7′	2.467	1.233	180.0	$-x, 1-y, -z$
O17−HO17···O17′	2.455	1.228	180.0	$-x, -y, -z$
O27−HO27···O40′	2.682	1.940	158.8	$1-x, -y, -z$
O31−H31A···O11	2.858	2.021	171.9	$x, y, 1+z$
O31−H31B···O15	3.001	2.216	149.7	x, y, z
O32−H32A···O12′	2.827	1.939	160.7	$x, y, 1+z$
O32−H32B···O15	3.146	2.534	134.9	x, y, z
O33−H33A···O1′	2.822	2.192	165.7	$1-x, 1-y, -z$
O33−H33B···O21′	2.828	1.909	168.9	$x, 1+y, z$
O34−H34A···O2	2.762	2.060	152.2	x, y, z
O34−H34B···O23	2.810	1.994	162.4	x, y, z
O35−H35A···O2′	2.837	2.030	167.3	$-x, 1-y, -z$
O35−H35B···O7	2.903	2.149	165.1	x, y, z
O36−H36A···O12′	2.867	1.835	163.8	$x,y,1+z$
O36−H36B···O33′	2.882	1.990	161.8	$-x, 1-y, 1-z$
O37−H37A···O4′	2.832	2.083	156.1	$x, y, -1+z$
O37−H37B···O46′	3.393	2.338	172.5	$-x, 1-y, -z$
O40−H40A···O37′	2.728	1.806	161.3	$1-x, -y, -1-z$
O40−H40B···O21	2.957	2.037	171.4	x, y, z
O41−H41A···O42′	3.338	2.161	141.9	$1+x, y, z$
O42−H42A···O46′	2.746	1.928	152.8	$-1-x, 1-y, 1-z$
O42−H42B···O22′	2.900	2.244	120.3	$-x, -y, -z$

structure. The hydrogen atoms on the terminal carboxylate oxygen atoms O(7) and O(17) sit on an inversion center of symmetry (resulting in a total occupancy of one), and through strong hydrogen-bonding interactions (see Table 3) they form chains of the anion of **1** running along the *b* axis (Figure 2). The other protonated terminal carboxylate oxygen, O(27), is hydrogen bonded to a lattice water molecule.

Six sodium counterions and 16 water molecules of crystallization per mononuclear anion are also present in the lattice of **1**. The sodium cations are in contact with the carboxylate oxygens of the citrate anions as well as the lattice water molecules at distances in the range 2.255(3)−2.566(3) Å. The sodium cations and the water solvent molecules are in contact with the carboxylate oxygens of the citrate ligands, establishing an extensive hydrogen-bonding network (Table 3) responsible for the stability of the crystal lattice in **1**.

By the same token, the terminal protonated carboxylate groups through strong hydrogen-bonding interactions are responsible for the development of the lattice structure of **2**.

Table 4. Hydrogen Bonds in 2

interaction	D···A (Å)	H···A (Å)	D−H···A (deg)	sym operation
O7−HO7···O7′	2.474	1.237	180.0	$-x, -y, 1-z$
O17−HO17···O17′	2.446	1.223	180.0	$1-x, -y, -z$
O27−HO27···O1′	2.575	1.461	165.2	$-x, 1-y, 1-z$
W1−HW1A···W6	2.807	1.952	170.7	x, y, z
W1−HW1B···O12′	2.692	1.915	178.8	$-1+x, 1+y, z$
W2−HW2A···O4′	2.903	2.054	175.2	$-x, 1-y, -z$
W2−HW2B···O24	2.970	2.059	159.0	x, y, z
W3−HW3A···O24′	3.026	2.261	165.5	$-1+x, y, z$
W3−HW3B···O12′	2.682	2.001	167.2	$-x, -y, -z$
W4−HW4A···O23′	2.886	1.906	160.2	$-x, 1-y, 1-z$
W5−HW5A···O11′	2.780	2.044	168.3	$-x, -y, 1-z$
W6−HW6A···O21′	2.749	1.990	158.4	$-1+x, y, z$
W7−HW7A···O14′	2.872	2.251	126.1	$-x, -y, -z$
W7−HW7B···O14	2.834	2.336	134.3	x, y, z
N1−HN1A···O11′	2.998	2.337	157.9	$x, 1+y, z$
N1−HN1B···O17′	2.877	1.765	163.2	$1-x, 1-y, -z$
N2−HN2A···O2′	2.850	2.135	166.7	$1-x, -y, 1-z$
N2−HN2B···O21	2.889	2.120	167.9	x, y, z
N2−HN2C···O14′	2.879	2.098	126.6	$1+x, y, z$
N2−HN2D···O7′	2.909	1.981	160.9	$1+x, y, z$
N3−HN3A···O3	3.049	2.297	141.7	x, y, z
N3−HN3B···O11	2.726	1.962	159.3	x, y, z
N3−HN3C···O22	2.929	2.205	135.2	x, y, z
N3−HN3D···O22′	2.942	2.104	171.3	$1-x, -y, 1-z$

The hydrogen atoms on the terminal carboxylate oxygen atoms O(7) and O(17) sit on an inversion center of symmetry (resulting in a total occupancy of one), and through strong hydrogen bonds (see Table 4) they form zigzag chains of the anion of **2** (Figure 3). The other protonated terminal carboxylate oxygen, O(27), is hydrogen bonded to a deprotonated terminal carboxylate group (O(1)). Thus, layers of the anion in **2** are formed parallel to the *bc* plane.

Three sodium and three ammonium counterions and nine water molecules of crystallization per mononuclear anion are also present in the lattice of **2**. The sodium cations are in contact with the carboxylate oxygens of the citrate anions as well the lattice water oxygens at distances in the range 2.256(6)−2.635(7) Å. The ammonium cations and the water solvent molecules are in contact with the carboxylate oxygens of the citrate ligands, establishing an extensive hydrogen-bonding network (Table 4) responsible for the stability of the crystal lattice in **2**.

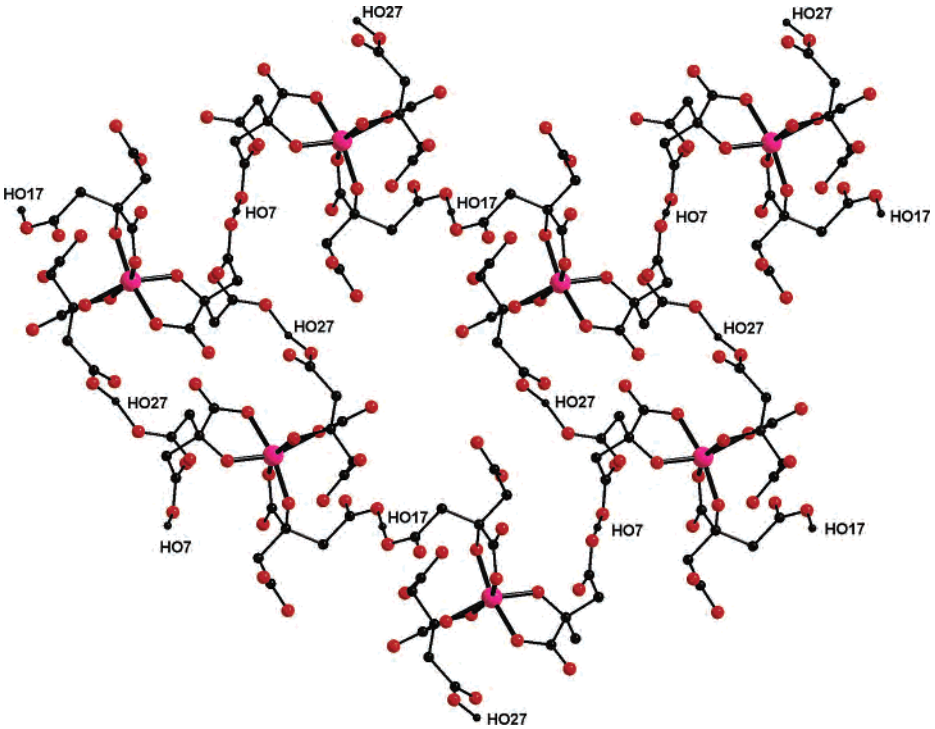

Figure 3. ORTEP plot of **2** showing the development of layers of the anions parallel to the *bc* plane through hydrogen-bonding interactions (open bonds through HO(27)).

FT-IR Spectroscopy. The FT-Infrared spectra of **1** and **2** in KBr revealed the presence of vibrationally active carboxylate groups. Antisymmetric as well as symmetric vibrations for the carboxylate groups of the coordinated citrate ligands dominated the spectrum. Specifically, antisymmetric stretching vibrations $\nu_{as}(COO^-)$ were present for the carboxylate carbonyls in the range 1653−1574 and 1631−1557 cm^{-1} for **1** and **2**, respectively. Symmetric vibrations $\nu_s(COO^-)$ for the same groups were present in the range 1436−1352 and 1421−1351 cm^{-1} for **1** and **2**, respectively. The frequencies of the observed carbonyl vibrations were shifted to lower values in comparison to the corresponding vibrations in free citric acid, indicating changes in the vibrational status of the citrate ligand upon coordination to the titanium ion.[20] The difference between the symmetric and antisymmetric stretches, $\Delta(\nu_{as}(COO^-)-\nu_s(COO^-))$, was greater than 200 cm^{-1}, indicating that the carboxylate groups of the citrate ligand were either free or coordinated to the metal ion in a monodentate fashion.[20,21] This was further confirmed by the X-ray crystal structures of **1** and **2**. All of the aforementioned assignments were in agreement with previous assignments in mononuclear $Ti^{IV}O_6$ complexes[22] and in line with prior reports on carboxylate containing ligands bound to different metal ions.[23−28]

Solid-State NMR Spectroscopy. The MAS ^{13}C NMR spectrum of **1** is consistent with the coordination mode of citrate around the Ti(IV) ion. The spectrum showed four separate peak features. Two of those lie in the high-field region whereas the other two appear in the low-field region. The broad peak(s) in the high-field region could be assigned to the two methylene carbons (42.8 ppm) located adjacent to the terminal carboxylates of the citrate ligand. The resonance at 89.6 ppm is reasonably attributed to the central carbon atom located adjacent to the bound central carboxylate group. In the low-field region, where the carbonyl carbon resonances are expected, there was only one peak observed (177.7 ppm) for the terminal carboxylate groups, both bound to the two Ti(IV) ions of the central core. There is also one peak observed (187.1 ppm) for the bound central carboxylate carbon of the citrate ligand. This signal is shifted to lower field by 10.5 ppm in comparison to the previous signal for the terminal carboxylate groups, most likely due to the presence of the nearby ionized alkoxide group. A similar pattern of ^{13}C resonances was observed in the case of mononuclear complexes such as $(NH_4)_5[Al(C_6H_4O_7)_2]\cdot$

(20) Deacon, G. B.; Philips, R. *J. Coord. Chem. Rev.* **1980**, *33*, 227−250.
(21) Djordjevic, C.; Lee, M.; Sinn, E. *Inorg. Chem.* **1989**, *28*, 719−723.
(22) Nakamoto, K. In *Infrared and Raman Spectra of Inorganic and Coordination Compounds, Part B*, 5th ed.; John Wiley and Sons: New York, 1997.
(23) (a) Matzapetakis, M.; Raptopoulou, C. P.; Terzis, A.; Lakatos, A.; Kiss, T.; Salifoglou, A. *Inorg. Chem.* **1999**, *38*, 618−619. (b) Matzapetakis, M.; Raptopoulou, C. P.; Tsohos, A.; Papefthymiou, B.; Moon, N.; Salifoglou, A. *J. Am. Chem. Soc.* **1998**, *120*, 13266−13267. (c) Matzapetakis, M.; Dakanali, M.; Raptopoulou, C. P.; Tangoulis, V.; Terzis, A.; Moon, N.; Giapintzakis, J.; Salifoglou, A. *J. Biol. Inorg. Chem.* **2000**, *5*, 469−474. (d) Matzapetakis, M.; Karligiano, N.; Bino, A.; Dakanali, M.; Raptopoulou, C. P.; Tangoulis, V.; Terzis, Giapintzakis, J.; Salifoglou, A. *Inorg. Chem.* **2000**, *39*, 4044−4051.
(24) Griffith, W. P.; Wickins, T. D. *J. Chem. Soc. A* **1968**, 397−400.
(25) Vuletic, N.; Djordjevic, C. *J. Chem. Soc., Dalton Trans.* **1973**, 1137−1141.
(26) Kaliva, M.; Giannadaki, T.; Raptopoulou,C. P.; Tangoulis, V.; Terzis, A.; Salifoglou, A. *Inorg. Chem.* **2001**, *40*, 3711−3718.
(27) Tsaramyrsi, M.; Kavousanaki, D.; Raptopoulou, C. P.; Terzis, A.; Salifoglou, A. *Inorg. Chim. Acta* **2001**, *320*, 47−59.
(28) Matzapetakis, M.; Kourgiantakis, M.; Dakanali, M.; Raptopoulou, C. P.; Terzis, A.; Lakatos, A.; Kiss, T.; Banyai, I.; Iordanidis, L.; Mavromoustakos, T.; Salifoglou, A. *Inorg. Chem.* **2001**, *40*, 1734−1744.

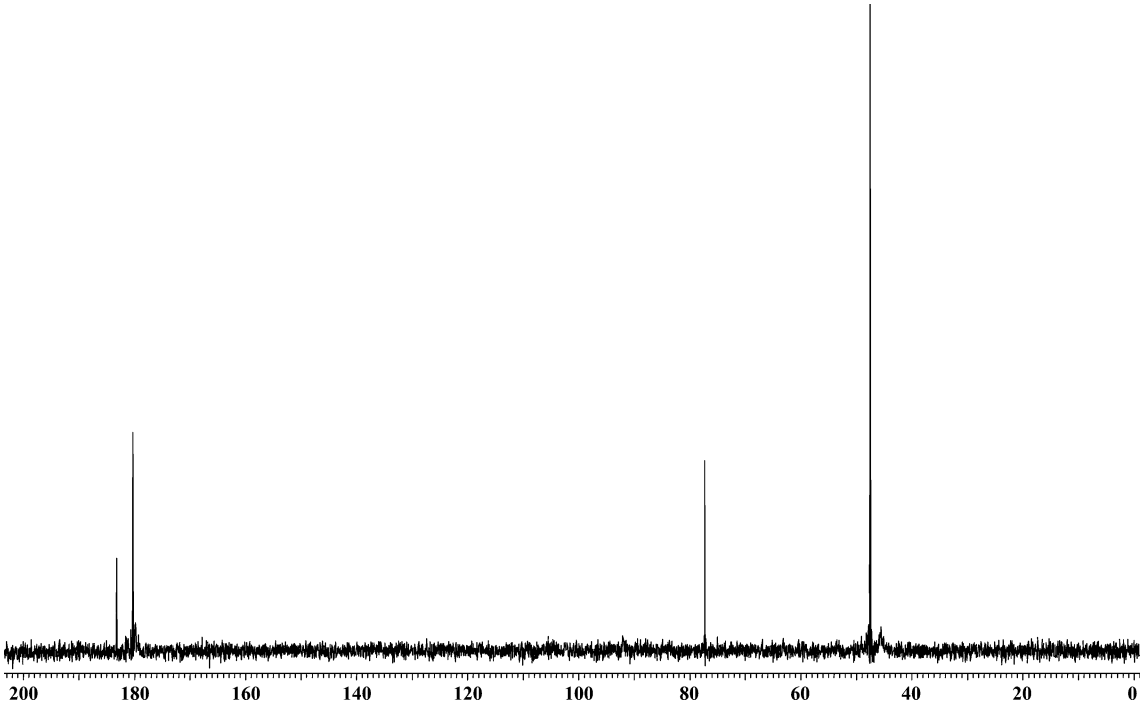

Figure 4. Solution ^{13}C NMR spectrum of $Na_6[Ti(C_6H_{4.5}O_7)_2(C_6H_5O_7)]\cdot 16H_2O$ (**1**) in D_2O.

$2H_2O$,[28] the tetranuclear complex $(NH_4)_8[Ti_4(C_6H_4O_7)_4(O_2)_4]\cdot 8H_2O$ (**7**),[11] and dinuclear complexes such as $Na_2[Bi_2(C_6H_4O_7)_2]\cdot 7H_2O$.[29] In the latter case, fully resolved resonances were observed for the carbons of the two variably bound CH_2COO^- groups (one is bound in a bidentate fashion to the bismuth ion, whereas the other one serves as a bridge to two bismuth ions).

Solution NMR Spectroscopy. The solution ^{13}C NMR spectrum of complex **1** was measured in D_2O (Figure 4). The spectrum revealed the presence of several resonances. There was one resonance in the high-field region (47.6 ppm), which was attributed to the CH_2 groups of the citrate ligands bound to the central Ti(IV) ion. The resonance at 77.3 ppm was assigned to the central carbon of the bound citrate. The signal at 180.3 ppm in the lower field region was assigned to the terminal carboxylate carbons coordinated to the Ti(IV) central ion. The resonance located at the low end of the field (183.2 ppm) was attributed to the central carboxylate carbon attached to the Ti(IV) ion. This signal was shifted to lower fields in comparison to the other signal belonging to the terminal carboxylate carbons. The shift was ~3.0 ppm downfield and was comparable to that observed in the MAS ^{13}C solid-state spectrum of **1**. In this case as well, the shift was most likely due to the presence of the central carboxylate carbon close to the deprotonated alkoxide group of the Ti(IV) coordinated citrates. It is worth noting that the pattern of resonances observed was similar to that observed in the solid state ^{13}C-MAS NMR spectrum of **1**. Therefore, there was a consistency between the solid and solution state spectra. Further inquiry into the solution ^1H NMR spectroscopy of compound **1** in D_2O reveals the presence of free citrate in equilibrium with the species under investigation (see Supporting Information). Collectively, the data in solution support the picture of the mononuclear complex provided by the solid-state NMR spectrum of **1**.

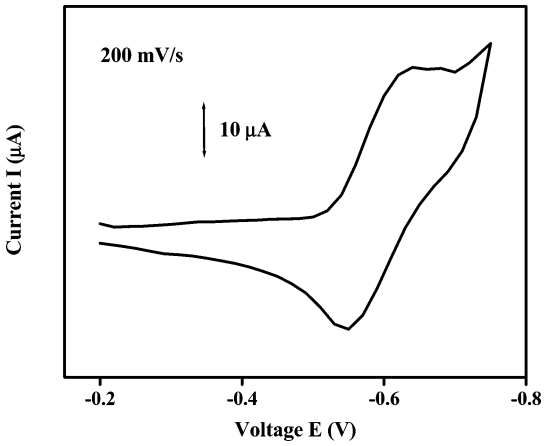

Figure 5. Cyclic voltammetric trace of $Na_3(NH_4)_3[Ti(C_6H_{4.5}O_7)_2(C_6H_5O_7)]\cdot 9H_2O$ (**2**) in water.

Cyclic Voltammetry. The cyclic voltammetry of complex **2** was studied in aqueous solution in the presence of KNO_3 as a supporting electrolyte. The cyclic voltammogram shows a quasi-reversible wave at $E_{1/2} = -0.6$ V vs SCE ($\Delta E = 98$ mV, $i_{pa}/i_{pc} < 1$, $i_{pc}/\{(\upsilon)^{1/2}C\}$ variable) that corresponds to the Ti(III)/Ti(IV) redox couple (Figure 5). The observed $E_{1/2}$ value is comparable to albeit lower than the one reported for Ti(III)−citrate preparations at pH 7. Attempts to pursue the isolation of the one-electron-reduced product of the title complex **2** are currently ongoing.

Discussion

Diverse Synthetic Chemistry of the Ti(IV)−Citrate Aqueous System. The current synthetic investigation ex-

(29) Barrie, P. J.; Djuran, M. I.; Mazid, M. A.; McPartlin, M.; Sadler, P. J.; Scowen, I. J.; Sun, H. *J. Chem. Soc., Dalton Trans.* **1996**, 2417−2422.

plored the reactivity of the aqueous binary $TiCl_4$−citric acid system at a specific pH value. In an expedient fashion, the two simple reagents under the influence of sodium hydroxide or sodium hydroxide and aqueous ammonia (1:1) afforded the mononuclear complexes $Na_6[Ti(C_6H_{4.5}O_7)_2(C_6H_5O_7)]\cdot 16H_2O$ (**1**) and $Na_3(NH_4)_3[Ti(C_6H_{4.5}O_7)_2(C_6H_5O_7)]\cdot 9H_2O$ (**2**). Analytical, spectroscopic, and finally X-ray crystallographic techniques revealed the identity of the new species at a near physiological pH value. As discrete species, complexes **1** and **2** arose out of aqueous media to project a very distinct picture of the mode of coordination of the three citrate ligands around the central metal ion and the concomitantly formulated octahedral geometry around it. Most important of all, however, was the variable protonation state of the bound citrate ligands around Ti(IV). Specifically, two of the bound citrates share a hydrogen atom with their neighbors, thus affording a 3.5− citrate anion $(C_6H_{4.5}O_7)^{3.5-}$, while the third one is triply deprotonated. In all cases, the site of protonation was the terminal carboxylates of the citrates bound to Ti(IV).

From the aqueous chemistry point of view in the binary system Ti(IV)−citrate, there appear to be other mononuclear octahedral structural units bearing the $Ti^{IV}O_6$ core with oxygens surrounding the central metal ion and belonging to citrate ligands. Such units include, apart from complexes **1** and **2**, the anionic complexes $[Ti(C_6H_6O_7)_3]^{2-}$,[13] $[Ti(C_6H_6O_7)_2(C_6H_5O_7)]^{3-}$, and $[Ti(C_6H_5O_7)_2(C_6H_6O_7)]$.[4−16] In light of these species, specific structural attributes of the series of available complexes and similarities and differences among them could be noted that bear relevance to their presence in the requisite speciation scheme(s). In particular, similarities include (a) mononuclear octahedral Ti(IV)−citrate species isolated and structurally characterized thus far, (b) Ti(IV)−citrate complexes in which the coordinated citrate ligands bind to the titanium ion through the central alkoxide and carboxylate groups in a consistent fashion, (c) bound citrate ligands in which the terminal carboxylate groups do not participate in the coordination sphere of titanium ion, and (d) sites of (de)protonation in all cases of bound citrates which are the terminal carboxylate groups. The major striking difference among the diverse spectrum of species available is the variable degree of protonation among the three bound citrates not only within the same complex but also within different species. This structural specificity toward the terminal carboxylate groups of citrates bound to metal ions was observed before and was the result of synthetic efforts unfolding under pH-dependent conditions affording variable degree of protonation ligands bound to metal ions with the same oxidation state.[28] As a consequence of this (de)protonation process, the charge on the corresponding complexes is different as one would expect.

Overall, it appears that the elaborated structural attributes are quite familiar features in metal ion citrate aqueous chemistry. Specifically, the synthetic chemistry between the early transition metal ion Ti(IV) and physiological ligands, like citric acid, offers a number of parallelisms with similar chemistries unfolding between citric acid and Ga(III), Al(III), Fe(III), Mn(II), and Mn(III). In the case of these metal ions, at their specified oxidations states, the aqueous synthetic chemistry developed as a function of pH has resulted in the isolation and characterization of anionic species such as $[Al(C_6H_4O_7)_2]^{5-}$,[23a] $[Al(C_6H_4O_7)(C_6H_5O_7)]^{4-}$,[28] $[Fe(C_6H_4O_7)_2]^{5-}$,[23b] $[Mn(C_6H_4O_7)_2]^{5-}$,[23d] and $[Mn(C_6H_5O_7)_2]^{4-}$.[23d] In all of these species, the presence of bound citrate ligands to the metal ions was a consistent structural feature, with the (de)protonation state of the citrate linked to the terminal carboxylate group not participating in the coordination sphere of the central metal ion. Especially intriguing appears to be the case of vanadium(V), an element abutting titanium in the periodic table, with the same electronic configuration (Ti(IV) vs V(V)). Thus, its aqueous chemistry with citric acid might be similar to the titanium chemistry in a number of different respects. As a matter of fact, that happens only in the case of the aqueous ternary peroxo−citrate systems of Ti(IV) and V(V) where stable dinuclear complexes arise.[30] An analogous chemistry does not develop with the nonperoxo binary systems Ti(IV)−citrate and V(V)−citrate, where octahedral mononuclear complexes form that exhibit diverse protonation states for the bound citrates around Ti(IV). One cannot unequivocally exclude the possibility that variable structure Ti(IV)−citrate species will be isolated in the future that will broaden the structural diversity in the binary Ti(IV)−citrate system.

Links to Ti(IV)−Citrate Speciation. The presence of complex **1** (or **2**) in aqueous solutions of the binary Ti(IV)−citrate system signifies its importance as a component of the system at near physiological pH values. Hence, its significance is tightly linked to the speciation of the requisite system in aqueous media. The aqueous speciation itself, however, is not presently available. Had it been available, it would have provided essential information on the distribution of potential species as a function of pH and the concentration of the two major reactants. In the absence of such information, complex **1** (and **2**) offer a vital link to the series of species presently known to exist as participants in the aqueous distribution of the Ti(IV)−citrate system. Given the pH-dependence of equilibria in a speciation scheme, the arisen series of complexes points out (a) the nature of complexes arising in such a distribution and (b) their structural diversity exemplified through (de)protonation processes, selectively occurring at the nonparticipating carboxylate terminals of the bound citrates around Ti(IV).

It is worth noting that the so far available data on the structural diversity of mononuclear octahedral Ti(IV)−citrate pH variants suggest sequential single proton abstractions from corresponding terminal carboxylate sites on bound citrates, without any concomitant coordination number, mode, or geometry changes. As a result, the charges on the sequentially arising species increase in steps of a single charge, starting from 2− and ending at 8−, covering overall a six proton process in the entire pH range under these conditions. The entire series projected on the aforementioned grounds includes several species (Figure 6). By no means is it implied that other species of variable nuclearity are not

(30) Kaliva, M.; Raptopoulou, C. P.; Terzis, A.; Salifoglou, A. *Inorg. Chem.* **2004**, *43*, 2895−2905.

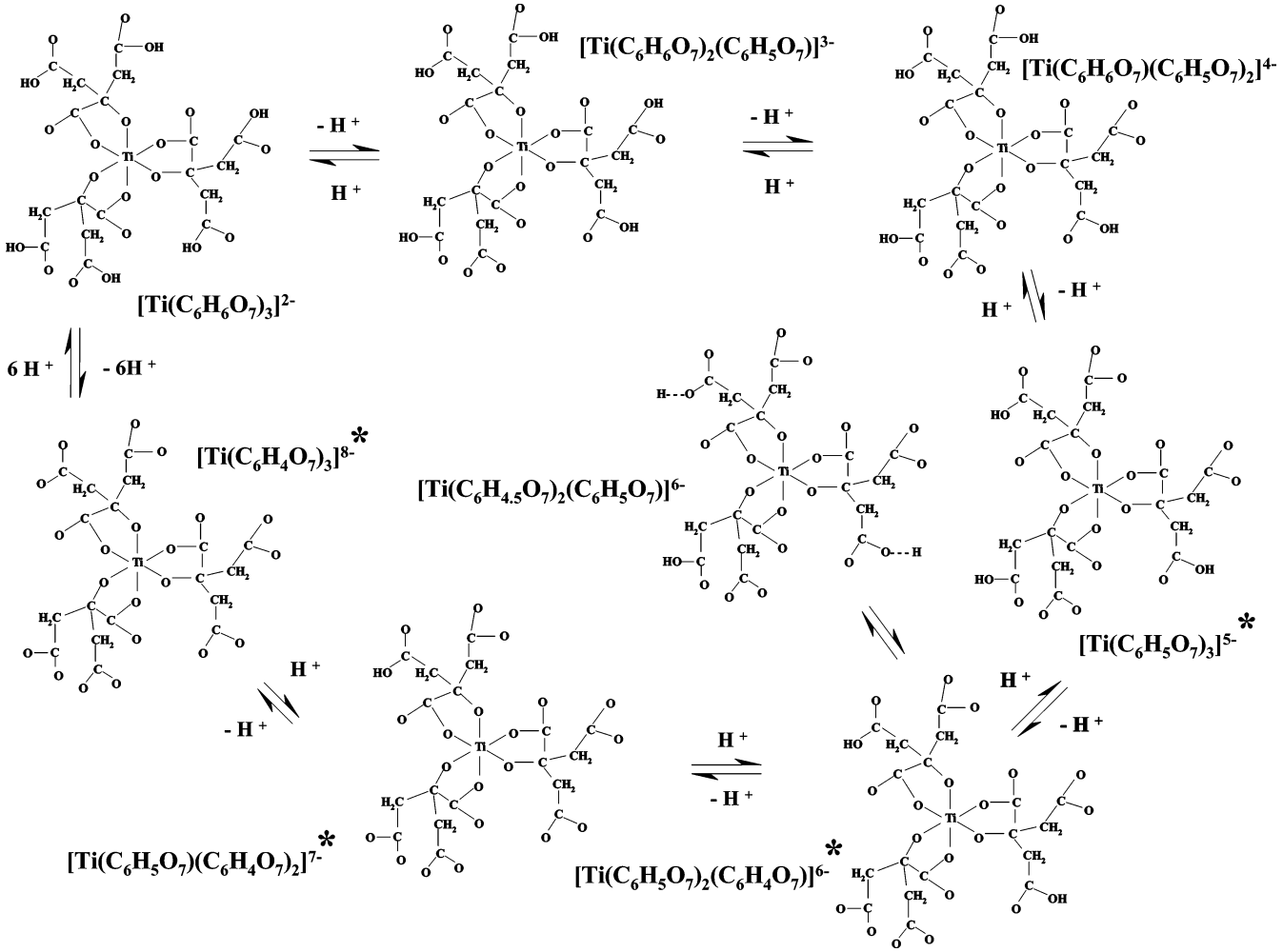

Figure 6. Potential aqueous speciation scheme encompassing mononuclear octahedral pH variants of Ti(IV)−citrate species. The sequential equilibria depicted reflect single-proton processes. The collective (de)protonation processes include 6 protons. Species marked with an asterisk represent Ti(IV)−citrate species that currently elude isolation and characterization.

present. Detailed synthetic and aqueous solution studies are crucial in delineating this dilemma. To the degree that the above-mentioned species are truly participants in the requisite speciation scheme, pertinent pH-dependent interconversion studies are needed. Such studies are currently ongoing.

Collectively, the synthetic efforts targeting Ti(IV)−citrate complexes from aqueous solutions have contributed to delineating the nature of a number of such species arising in the course of pH-dependent reactions. Each such well-characterized species reflects the power of synthetic chemistry in delivering isolated, structurally and spectroscopically characterized Ti(IV)−tricitrate complexes, as potential participants of the requisite speciation scheme. To this end, the chemistry of the binary system Ti(IV)−citrate emphasizes the dominance of tricitrate chelate complexes of titanium(IV) ion as key species in the aqueous solutions of that binary system. Moreover, it offers detailed physicochemical information which would help establish the basis of understanding potential interactions of Ti(IV) with biologically relevant molecules. The nature and details of these interactions are crucial, with solubility and bioavailability of aqueous titanium forms being key potential contributors into (bio)chemical pathways leading to clinical symptoms, already described at the clinical level. In this regard, potential roles for titanium (pure or in alloys and composites) have been suggested, covering protein expression,[31] growth factor recruitment,[32] signal transduction,[33] enzyme activation,[34] gene expression,[35] and others.[36]

With awareness of the intricate nature of the arisen interactions and potential effects in biological loci, the herein presented complexes **1** and **2** represent a token of the work needed to understand (a) the chemistry of the interactions of titanium with physiological ligands and (b) the concomitant biological implications. These goals are now being pursued in our laboratories.

(31) Bledsoe, J. G.; Slack, S. M. *J. Biomater. Sci., Polym. Ed.* **1998**, *9*, 1305−1312.
(32) Frenkel, S. R.; Simon, J.; Alexander, H.; Dennis, M.; Ricci, J. L. *J. Biomed. Mater. Res.* **2002**, *63*, 706−713.
(33) Vermes, C.; Roebuck, K. A.; Chandrasekaran, R.; Dobai, J. G.; Jacobs, J. J.; Glant, T. T. *J. Bone Miner. Res.* **2000**, *15*, 1756−1765.
(34) Palmbos, P. L.; Sytsma, M. J.; DeHeer, D. H.; Bonnema, J. D. *J. Orthop. Res.* **2002**, *20*, 483−489.
(35) (a) Kapanen, A.; Kinnunen, A.; Ryhanen, J.; Tuukkanen, J. *Biomaterials* **2002**, *23*, 3341−3346. (b) Kwon, S. Y.; Lin, T.; Takei, H.; Ma, Q.; Wood, D. J.; O'Connor, D.; Sung, K. L. *Biorheology* **2001**, *38*, 161−183.
(36) Guo, M.; Sun, H.; McArdle, H. J.; Gambling, L.; Sadler, P. J. *Biochemistry* **2000**, *39*, 10023−10033.

Acknowledgment. This work was supported by the Department of Chemical Engineering, Aristotle University of Thessaloniki, the Chemical Process Engineering Research Institute, Thermi, and the Department of Chemistry, University of Crete, Heraklion, Greece.

Supporting Information Available: X-ray crystal crystallographic files, in CIF format, and listings of positional and thermal parameters and H-bond distances and angles for **1** and **2**. The material is available free of charge via Internet at http://pubs.acs.org.

IC049276O